

# Optimal wavelength for radio polarization observations

Tigran G. Arshakian<sup>1</sup>\* and Rainer Beck<sup>1</sup>

Max-Planck-Institut für Radioastronomie, Auf dem Hügel 69, 53121 Bonn, Germany  
e-mail: [tarshakian;rbeck]@mpi-fr-bonn.mpg.de

Received ...; accepted ...

## ABSTRACT

**Aims.** Polarized radio synchrotron emission from interstellar, intracluster and intergalactic magnetic fields is affected by wavelength-dependent Faraday depolarization. The maximum polarized intensity depends on the physical properties of the depolarizing medium. New-generation radio telescopes like LOFAR, SKA and its precursors need a wide range of frequencies to cover the full range of objects.

**Methods.** The optimum wavelength of maximum polarized intensity (PI) is computed for the cases of depolarization in magneto-ionic media including regular magnetic fields (differential Faraday rotation) or turbulent magnetic fields (internal or external Faraday dispersion).

**Results.** Polarized emission from bright galaxy disks, spiral arms and cores of galaxy clusters are best observed at centimeter wavelengths, halos of galaxies and clusters at decimeter wavelengths. Intergalactic filaments need observations at meter wavelengths. Measurement of the PI spectrum allows us to derive the average Faraday rotation measure  $|RM|$  or its dispersion, without knowledge of polarization angles, if the medium has a simple structure. Periodic fluctuations in PI at low frequencies are a signature of differential Faraday rotation. Internal and external Faraday dispersion can be distinguished by the different slopes of the PI spectrum at low frequencies.

**Key words.** Techniques: polarimetric – ISM: magnetic fields – galaxies: clusters: general – galaxies: halos – galaxies: magnetic fields – radio continuum: galaxies

## 1. Introduction

Many astrophysical sources reveal a power-law synchrotron spectrum with an almost constant spectral index over a wide radio frequency range. The total intensity of synchrotron emission depends on the number density of cosmic-ray electrons and the strength of the total magnetic field component normal to the line-of-sight of the observer, while the polarized intensity is related to ordered magnetic fields. Ordered fields can be regular (coherent), generated by the mean-field dynamo (Beck et al. 1996) or anisotropic, generated from turbulent magnetic fields by compressing or shearing gas flows. Turbulent fields with random orientations give rise to unpolarized synchrotron emission. The degree of synchrotron polarization is a function of the ratio between ordered and turbulent fields (Sokoloff et al. 1998).

The intensity of polarized radio continuum emission is the result of competition between two processes: synchrotron emission and Faraday depolarization, both of which increase with wavelength. The polarization plane changes by Faraday rotation when the radio wave passes through a magneto-ionic

medium with regular magnetic fields. If the region contains cosmic-ray electrons, thermal electrons and regular magnetic fields, the polarization planes from waves from the far side of the emitting layer are more rotated than those from the near side.

Faraday rotation in a magnetized plasma is an important signature of magneto-ionic media containing regular magnetic fields and a measure of field strength and thermal electron density. To determine Faraday rotation measures (RM), defined as  $\Delta\chi = RM \Delta\lambda^2$ , polarization angles  $\chi$  need to be measured at several wavelengths. Faraday rotation in a foreground screen in front of the synchrotron-emitting region can be described by a single RM value which is constant over a wide wavelength range. If Faraday rotation occurs in the emitting region, the observable RM is no longer constant, and the concept of “Faraday depth” needs to be applied (Burn 1966). “RM Synthesis” Fourier-transforms the complex polarized intensity in many channels over a large frequency spread into a “Faraday spectrum” in Faraday depth space (Brentjens & de Bruyn 2005, Heald 2009). Emitting & rotating layers with simple distributions of the regular field and thermal electrons (“Burn’s slab”) can still be characterized by a mean RM (Sokoloff et al. 1998), as assumed in this paper.

Internal Faraday rotation in a synchrotron-emitting medium causes wavelength-dependent Faraday depolarization

Send offprint requests to: T.G. Arshakian

\* On leave from the Byurakan Astrophysical Observatory, Aragatsotn prov. 378433, Armenia, and Isaac Newton Institute of Chile, Armenian Branch

(DP) which is called differential Faraday rotation (DFR). Turbulent fields also cause wavelength-dependent depolarization (Faraday dispersion). Internal Faraday dispersion (IFD) occurs in an emitting and Faraday-rotating region, while external Faraday dispersion (EFD) may occur in a non-emitting foreground screen (Burn 1966, Sokoloff et al. 1998). DFR is a function of RM and wavelength (Eq. (4)), while Faraday dispersion depends on RM dispersion and wavelength (Eqs. (8) and (9)).

The spectrum of polarized intensity is a power law over a limited frequency range and often reveals a maximum at a certain wavelength  $\lambda_{max}$  (Conway et al. 1974, Tabara & Inoue 1980). Below  $\lambda_{max}$ , the degree of polarization decreases with decreasing wavelength, called “polarization inversion”. In the case of compact radio sources, polarization inversion is often related to flat-spectrum (opaque) sources and is probably caused by Faraday dispersion (Conway et al. 1974).

Depolarization of the emission from various cosmic objects varies strongly and depends on coherence length, strength of the regular and turbulent magnetic fields and thermal electron density. Hence, each population of polarized objects should be studied at the optimum wavelength at which the polarized intensity is maximum. In advent of the major polarization surveys planned with the future radio facilities like the Square Kilometre Array (SKA), its precursor telescopes ASKAP and MeerKAT, and low-frequency radio telescopes such as LOFAR and MWA, operating at different frequencies and having large bandwidths, it is crucial to identify the optimal frequency band (Section 2). In this paper, we also explore possibilities to distinguish between internal/external Faraday dispersion and differential Faraday rotation, which allows to investigate the physical properties of the depolarizing medium.

## 2. Optimal wavelength for maximum polarized intensity

The total intensity of the synchrotron emission detected in the rest frame of the observer at a frequency  $\nu$  is

$$I_\nu = C_1 n_{CR} B_{t,\perp}^{2(1+\alpha)} \nu^{-\alpha} L, \quad (1)$$

where  $n_{CR}$  is the density of cosmic-ray electrons (per energy interval) which have a power-law energy spectrum ( $N(E) \propto E^{-\gamma}$ ) with the spectral index  $\gamma$ , leading to the synchrotron spectral index  $\alpha = (\gamma - 1)/2$ .  $L$  is the linear size of the emitting region, and  $B_{t,\perp}$  is the strength of the total magnetic field perpendicular to the line of sight.

The polarized intensity is given by

$$P_\nu = p_0 I_\nu \frac{B_{ord,\perp}}{B_{t,\perp}} DP_\nu, \quad (2)$$

where  $p_0 = (1 + \gamma)/(7/3 + \gamma)$  is the maximum degree of polarization ( $p_0 \simeq 0.74$  for a typical spectral index of  $\gamma \simeq 2.7$  in galaxies),  $B_{ord,\perp}$  is the strength of the ordered (regular + anisotropic<sup>1</sup>) magnetic field perpendicular to the line of sight

<sup>1</sup> An anisotropic field can be generated by compressing or shearing an isotropic turbulent field; it contributes to polarized emission but not to Faraday rotation.

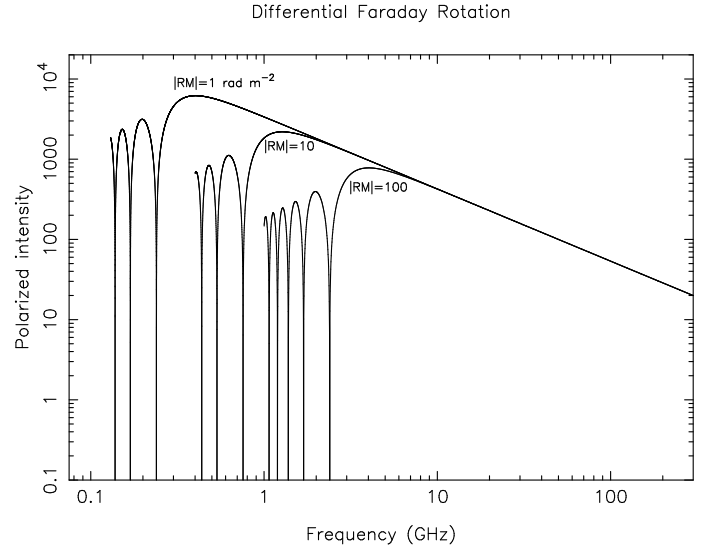


**Fig. 1.** Polarized intensity for a spectral index of total synchrotron intensity of  $\alpha = 0.9$  and depolarization by differential Faraday rotation at the level of  $|RM| = 1, 10$  and  $100 \text{ rad m}^{-2}$ .

and  $DP_\nu$  is the depolarization coefficient. Assuming that the cosmic-ray density, total and ordered magnetic fields are stationary, we write

$$P_\nu = C \nu^{-\alpha} DP_\nu, \quad (3)$$

where  $C = C_1 p_0 n_{CR} B_{ord,\perp}^2 B_{t,\perp}^{\alpha-1}$ .

### 2.1. Differential Faraday rotation

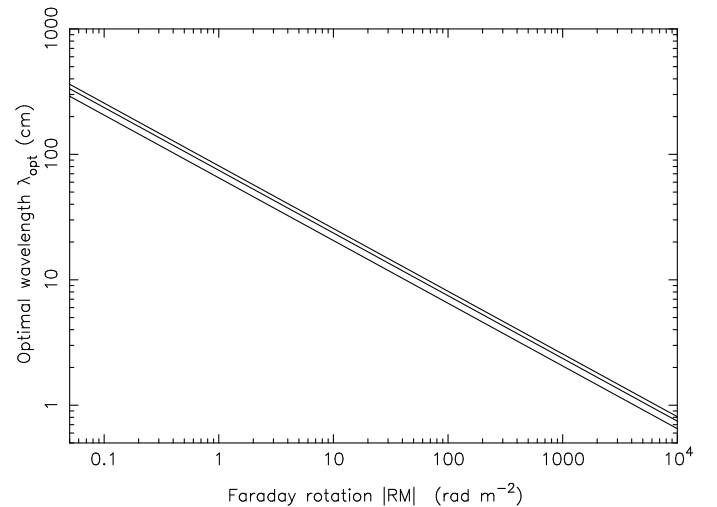


**Fig. 2.** Optimum wavelength of maximum polarized emission for a synchrotron spectrum with spectral index  $\alpha = 0.5, 0.9$  and  $1.3$  (from bottom to top) and depolarization by differential Faraday rotation as a function of  $|RM|$ .

Wavelength-dependent Faraday depolarization occurs in a region containing cosmic-ray electrons, thermal electrons and regular magnetic fields. The polarization planes of the waves from different synchrotron-emitting layers are rotated differently: the polarization planes from the near emitting layers rotate less than those emitted from the far layers. This effect is known as *differential Faraday rotation (DFR)* and is given by

$$DP = \frac{|\sin(2RM\lambda^2)|}{|2RM\lambda^2|}. \quad (4)$$

RM is the average observed rotation measure (in radians per square meter),

$$RM [\text{rad m}^{-2}] = 0.81 \int n_e B_{\text{reg}, \parallel} dL \approx 0.81 \langle n_e \rangle \langle B_{\text{reg}, \parallel} \rangle L, \quad (5)$$

where  $n_e$  (in  $\text{cm}^{-3}$ ) is the thermal electron density,  $B_{\text{reg}, \parallel}$  (in  $\mu\text{G}$ ) is the strength of the regular magnetic field along the line of sight, and  $L$  is the pathlength through the regular field and thermal gas in parsecs ( $pc$ ). We assume here that the magneto-ionic medium can be characterized by one single RM value, i.e. the distributions of  $n_e$  and  $B_{\text{reg}, \parallel}$  are smooth and symmetric along the line of sight (Sokoloff et al. 1998).

The maximum polarized intensity is reached at larger frequencies for larger values of RM (Fig. 1). At low frequencies (before the maximum) the slope of the curve, measured between 1/10 and 1/100 of the maximum polarized intensity, is  $\alpha \approx 100$  (Fig. 1). The periodic changes of  $DP$  with wavelength (Eq. (4)) lead to total depolarization at certain wavelengths, observable as “depolarization canals” in maps of polarized emission (e.g. Fletcher & Shukurov 2006). However, “canals” can also originate from steep gradients in polarization angle caused e.g. by turbulent fields (Sun et al. 2011).

Accounting the differential Faraday depolarization (Eq. (4)) and solving the equation  $dP_{\nu}/d\lambda = 0$ , we derive a transcendental equation for the optimal wavelength ( $\lambda_{\text{opt}}$ ) of the maximum polarized emission,

$$|\sin k| - \frac{2k}{2 - \alpha} |\cos k| = 0, \quad (6)$$

where  $k = 2|RM|\lambda_{\text{opt}}^2$ . The dependence of the optimal wavelength on rotation measure for  $\alpha = 0.5, 0.9$  and  $1.3$  is shown in Fig. 2: polarized sources with larger  $|RM|$  are best observed at smaller wavelengths,

$$\lambda_{\text{opt}} = A(\alpha) |RM|^{-0.5}. \quad (7)$$

If  $\lambda_{\text{opt}}$  is measured in  $m$ ,  $A(\alpha)$  is 0.65, 0.75, 0.81 for  $\alpha = 0.5, 0.9, 1.3$ .

Note that regions with thermal electrons and a constant regular field, but without cosmic-ray electrons (no synchrotron emission), called “Faraday screens”, cause Faraday rotation of polarized emission from background sources, but do not depolarize. Any variation of strength or direction of the regular field within the volume traced by the telescope beam causes RM gradients and hence depolarization (Burn 1966, Sokoloff et al. 1998) which is similar to external Faraday dispersion (see below).

## 2.2. Faraday dispersion

Depolarization by *internal Faraday dispersion (IFD)* occurs in a region containing cosmic-ray electrons, thermal electrons and turbulent magnetic fields and is given by

$$DP = \frac{1 - e^{-S}}{S}, \quad (8)$$

where  $S = 2\sigma_{\text{RM}}^2 \lambda^4$ . Depolarization by *external Faraday dispersion (EFD)* in a non-emitting Faraday screen is given by

$$DP = e^{-S}. \quad (9)$$

The observed dispersion of the RM in a simplified model of the turbulent magneto-ionic medium is,

$$\sigma_{\text{RM}}^2 = (0.81 n_e B_{\text{turb}} d)^2 f L / d \cong (0.81 \langle n_e \rangle \langle B_{\text{turb}} \rangle)^2 L d / f, \quad (10)$$

where  $n_e$  (in  $\text{cm}^{-3}$ ) is the electron density within the turbulent cells of size  $d$  (the “correlation length”, in  $pc$ ),  $\langle n_e \rangle$  is the average electron density along the pathlength  $L$  (in  $pc$ ),  $f$  is the filling factor of the cells ( $f = \langle n_e \rangle / n_e$ ) and  $\langle B_{\text{turb}} \rangle$  (in  $\mu\text{G}$ ) is the mean strength of the turbulent magnetic field, assumed to be the same inside and outside of the cells. We further assume that the field direction is constant within each cell.

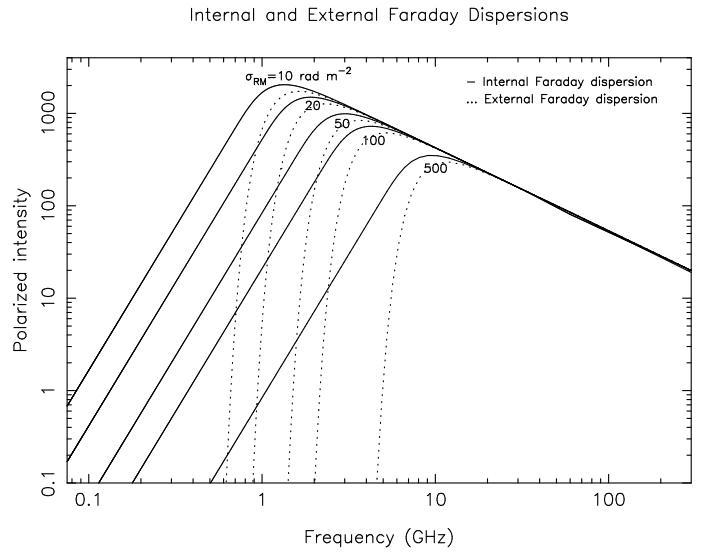


**Fig. 3.** Polarized intensity for a spectral index of total synchrotron intensity of  $\alpha = 0.9$  and depolarization by internal (solid line) and external (dashed line) Faraday dispersions at different levels of  $\sigma_{\text{RM}}$ .

Note that other definitions of  $\sigma_{\text{RM}}$  in the literature used a different dependence on the filling factor  $f$ . Future high-resolution radio observations are needed which can directly measure  $\sigma_{\text{RM}}$ .

The effect of depolarization of the polarized intensity by internal and external Faraday dispersions is shown in Fig. 3 for  $\alpha = 0.9$ . The dependence of polarization intensity on wavelength is the same for both mechanisms at high frequencies

where no depolarization occurs, while beyond the peak (at low frequencies) the polarized intensity decreases faster in the case of external Faraday dispersion. At low frequencies (before the maximum) the slopes of internal and external Faraday dispersion curves are significantly different: the spectrum is a power-law ( $P_\nu \propto \nu^{4-\alpha}$ ) for internal Faraday dispersion, while for external Faraday dispersion it deviates from a power law. The slope of the latter is estimated to be  $\alpha \simeq 15$  between 1/10 and 1/100 of the maximum polarized intensity. The intensity fixed at the level of  $\sigma_{\text{RM}}$  reaches the peak at a slightly larger frequency for external Faraday dispersion than in the case of internal Faraday dispersion (Fig. 3).

The equation for the optimal wavelength ( $\lambda_{\text{opt}}$ ) of maximum polarized emission in the case of internal RM dispersion is,

$$e^{2S_o} - \frac{8S_o}{\alpha - 4} - 1 = 0, \quad (11)$$

where  $S_o = 2\sigma_{\text{RM}}^2 \lambda_{\text{opt}}^4$ . For external RM dispersion we derive the equation,

$$\lambda_{\text{opt}} = \left( \frac{\alpha}{8\sigma_{\text{RM}}^2} \right)^{1/4}, \quad (12)$$

where  $\lambda_{\text{opt}}$  is measured in  $m$ .

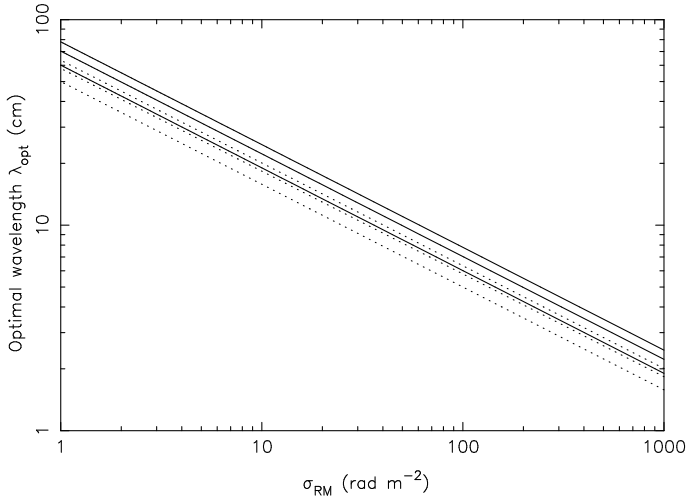


**Fig. 4.** Optimum wavelength of maximum polarized emission for a synchrotron spectrum with spectral index  $\alpha = 0.5, 0.9$  and  $1.3$  (from bottom to top) and depolarized by internal (solid line) and external (dashed line) Faraday dispersions against RM dispersion.

The dependence of the optimal wavelength on internal dispersion (full line) and external (dotted line) dispersion is shown in Fig. 4 for  $\alpha = 0.5, 0.9$  and  $1.3$ . Polarized sources with larger  $\sigma_{\text{RM}}$  are best observed at smaller wavelengths. In the case of internal RM dispersion we found that  $\lambda_{\text{opt}} = A_1 \sigma_{\text{RM}}^{-0.5}$ , where  $A_1 = 0.6, 0.7, 0.87$  for  $\alpha = 0.5, 0.9, 1.3$ . For external RM dispersion the relations are  $\lambda_{\text{opt}} = A_2 \sigma_{\text{RM}}^{-0.5}$ , where  $A_2 = 0.50, 0.58, 0.63$  for  $\alpha = 0.5, 0.9, 1.3$ .

At long wavelength and/or large Faraday dispersion ( $S \gg 1$ ) Eq. (9) can no longer be applied because the correlation length of polarized emission is smaller than the cell size  $d$  (Tribble 1991, Sokoloff et al. 1998), and the external depolarization by external dispersion becomes

$$DP = (2\sigma_{\text{RM}} \lambda^2)^{-1}. \quad (13)$$

This equation is valid only at wavelengths much longer than the optimum wavelength which corresponds to  $S_o = \alpha/4 < 1$  (see Eq. 12) and hence does not affect the results presented above.

### 2.3. Mixed cases

Many astrophysical media contain both regular and turbulent magnetic fields, while the descriptions of Faraday depolarization in Sections 2.1 and 2.2 are only valid if one type of magnetic fields dominates. In mixed cases with similar field strengths the total depolarization can still be described by Eq. (8) where  $S$  becomes a complex number (Sokoloff et al. 1998). As an approximation, it may be assumed that some fraction of the emitting medium on the far side is totally depolarized by Faraday dispersion and the remaining volume on the near side is subject to depolarization by differential Faraday rotation. Here, the total depolarization is the product of Eqs. (4) and (8) with appropriate weighting according to the strengths of the regular and turbulent field components.

## 3. Discussion and conclusions

Planning polarization observations needs to investigate the expected range of  $|RM|$  and Faraday dispersion (Table 1). The polarized emission of the inner disks, spiral arms, central regions of galaxies and the cores of galaxy clusters should be observed at wavelengths below a few centimeters (frequencies beyond about 10 GHz), in order to avoid strong depolarization by DFR and IFD. Outer galaxy disks, galaxy halos, halos of galaxy clusters and intergalactic filaments have lower RM and Faraday dispersion and are best observed at long wavelengths (Table 1). Polarized intensity from intergalactic filaments is very low because the predicted magnetic fields are weak, but increases due to the synchrotron spectrum towards the meterwave range where Faraday depolarization is still small. Observations with low-frequency telescopes such as LOFAR are most promising. Note, however, that the contribution of the fluctuating polarized emission of the Galactic foreground strongly increases towards low frequencies (Sun & Reich 2009).

The observed  $|RM|$  and RM dispersion reduce with redshift as  $(1+z)^{-2}$ . Thus the optimal wavelength to observe distant polarized sources is larger. The optimal frequency to observe a nearby bright galaxy disk with  $|RM|(z=0) = 200 \text{ rad m}^{-2}$  is  $\simeq 5 \text{ cm}$  (6 GHz, see Table 1). If we want to observe the same source, for example, at  $z=3$  then the observed  $|RM|(z=3) = 200/16 \simeq 12 \text{ rad m}^{-2}$  and the optimal wavelength for observation is about 21 cm (1.4 GHz). The optimal wavelength to observe a cluster core with  $\sigma_{\text{RM}}(z=0) \simeq 1000 \text{ rad m}^{-2}$  (Table 1) at  $z=3$  is about 7 cm (4 GHz). Hence, cluster cores and bright disk galaxies at high redshifts can be detected with ASKAP and the high-frequency SKA array.

If RMs of polarized background sources should be measured, DFR and IFD only occur in the sources and are generally low due to the small source sizes. EFD in the Galactic foreground with an RM dispersion of about  $10 \text{ rad m}^{-2}$  at high Galactic latitudes (Sun & Reich 2009) yields an optimal observation wavelength of about 20 cm. The all-sky RM surveys of the SKA (Gaensler et al. 2004) and of its pathfinder ASKAP (*POSSUM*; Gaensler et al. 2010) are planned in this frequency range. At low Galactic latitudes the RM dispersion is  $60\text{--}160 \text{ rad m}^{-2}$ , and the optimum wavelength is 5–7 cm.

In this paper we demonstrated that measurement of the spectrum of polarized intensity (PI) around the optimum wavelength offers another method to measure  $|RM|$  or Faraday dispersion, without measuring polarization angles. No absolute calibration of polarization angles and no correction for ionospheric Faraday rotation is needed here. However, if the emitting and rotating medium has a complicated structure, a spectrum of RM components in Faraday depth space is expected and the PI spectrum will also become complicated. A model for two components was discussed by Farnsworth et al. (2011).

Moreover, the knowledge of the optimum wavelength and hence the main (first) maximum of the PI spectrum is important for performing RM Synthesis. It is presumed that range around optimum wavelength is included in the observed spectral range to ensure the recovery of the main peak of the RM Transfer Function which is needed to clean the Faraday spectrum (Heald 2009).

We also showed that the slope of the PI spectrum at low frequencies is much steeper for EFD than for IFD (Fig. 4). This allows us to distinguish between these two effects, which is hardly possible with other methods. DFR has a similarly steep spectrum as EFD, but is easily recognizable by its periodic fluctuations, leading to total depolarization at certain wavelengths (Fig. 1).

**Acknowledgements.** This work was supported by the European Community Framework Programme 6, Square Kilometre Array Design Study (SKADS). TGA acknowledges support by DFG–SPP project under grant 566960. We thank Luigina Feretti and Torsten Enßlin for help in compiling cluster data for Table 1, as well as Wolfgang Reich, Rodion Stepanov and Dmitry Sokoloff for useful discussions.

## References

- Beck, R. 2005, in *Cosmic Magnetic Fields*, eds. R. Wielebinski & R. Beck, Springer, Berlin, p. 43
- Beck, R. 2007, *A&A*, 470, 539
- Beck, R., Brandenburg, A., Moss, D., Shukurov, A., & Sokoloff, D. 1996, *Ann. Rev. Astron. Astrophys.*, 34, 155
- Burn, B. J. 1966, *MNRAS*, 133, 67
- Conway, R. G., Haves, P., Kronberg, P. P., et al. 1974, *MNRAS*, 168, 137
- Farnsworth, D., Rudnick, L. & Brown, S. 2011, *ApJ*, in prep.
- Feain, I. J., Ekers, R. D., Murphy, T., et al. 2007, *ApJ*, 707, 114
- Fletcher, A. & Shukurov, A. 2006, *MNRAS*, 371, L21
- Fletcher, A., Berkhuijsen, E. M., Beck, R. & Shukurov, A. 2004, *A&A*, 414, 53
- Fletcher, A., Beck, R., Shukurov, A., Berkhuijsen, E. M. & Horellou, C. 2011, *MNRAS*, in press
- Gaensler, B. M., Beck, R., & Feretti, L. 2004, *New Astr. Rev.*, 48, 1003
- Gaensler, B. M., Landecker, T. L. & Taylor, A. R. 2010, *BAAS*, 42, 470
- Heald, G. 2009, in *Cosmic Magnetic Fields: From Planets, to Stars and Galaxies*, eds. K. G. Strassmeier et al., Cambridge Univ. Press, Cambridge, p. 591
- Heesen, V., Krause, M., Beck, R. & Dettmar, R.-J. 2009, *A&A*, 506, 1123
- Hummel, E., Beck, R. & Dahlem, M. 1991, *A&A*, 248, 23
- Kim, K.-T., Kronberg, P. P., Dewdney, P. E. & Landecker, T. L. 1990, *ApJ*, 355, 29
- Laing, R. A., Bridle, A. H., Parma, P. & Murgia, M. 2008, *MNRAS*, 391, 521
- Murgia, M., Govoni, F., Feretti, L., et al. 2004, *A&A*, 424, 429
- Sokoloff, D. D., Bykov, A. A., Shukurov, A., et al. 1998, *MNRAS*, 299, 189, and Erratum in *MNRAS*, 303, 207
- Sun, X. H. & Reich, W. 2009, *A&A*, 507, 1087
- Sun, X. H., Reich, W., Han, J. L., et al. 2011, *A&A*, 527, A74
- Tabara, H. & Inoue, M. 1980, *A&AS*, 39, 379
- Tribble, P. C. 1991, *MNRAS*, 250, 726
- van Weeren, R. J., Röttgering, H. J. A., Brüggen, M. & Hoeft, M. 2010, *Science*, 330, 347
- Vogt, C. & Enßlin, T. A. 2005, *A&A*, 434, 67
- Xu, Y., Kronberg, P. P., Habib, S. & Dufton, Q. W. 2006, *ApJ*, 637, 19

**Table 1.** Typical properties of astrophysical media which can be characterized by a single  $|RM|$  component and a RM dispersion  $\sigma_{RM}$ , and the corresponding optimum wavelengths for polarization observations, assuming a synchrotron spectral index  $\alpha = 0.9$

| Source  | $\langle n_e \rangle$<br>(cm <sup>-3</sup> ) | $B_{\text{reg}}$<br>( $\mu\text{G}$ ) | $B_{\text{turb}}$<br>( $\mu\text{G}$ ) | $L$<br>(pc)                    | $d$<br>(pc)          | $f$  | Ref.  | $ RM ^a$<br>(rad m <sup>-2</sup> ) | $\lambda_{\text{opt}}^b$<br>(cm) | $\sigma_{RM}^a$<br>(rad m <sup>-2</sup> ) | $\lambda_{\text{opt}}^c$<br>(cm) |
|---|--|---------------------------------------|--|--------------------------------|----------------------|------|-------|------------------------------------|----------------------------------|---|----------------------------------|
| <b>Emitting &amp; Faraday-rotating media</b>                    |  |                                       |  |                                |                      |      |       |                                    |                                  |   |                                  |
| Faint galaxy disk   | 0.01   | 5                                     | 5                                      | 1000                           | 50                   | 0.2  | 1     | 40                                 | 12                               | 20  | 13                               |
| Bright galaxy disk  | 0.05   | 5                                     | 10                                     | 1000                           | 50                   | 0.5  | 2,3   | 200                                | 5                                | 130                                       | 5                                |
| Spiral arm  | 0.1  | 2                                     | 20                                     | 500                            | 50                   | 0.5  | 3     | 80                                 | 8                                | 360                                       | 3                                |
| Star-forming complex  | 0.5  | < 2                                   | 20                                     | 100                            | 10                   | 0.05 | 3     | < 80                               | > 8                              | 1100                                      | 2                                |
| Faint galaxy halo   | 0.01   | 1                                     | 3                                      | 1000                           | 50                   | 0.5  | 4     | 8                                  | 26                               | 8   | 20                               |
| Bright galaxy halo  | 0.02   | 3                                     | 5                                      | 1000                           | 50                   | 0.5  | 4,5   | 50                                 | 11                               | 25  | 12                               |
| Cluster halo  | 0.001  | < 1                                   | 1-5                                    | 10 <sup>5</sup>                | 1-5 10 <sup>4</sup>  | 1?   | 6,7   | < 80                               | > 8                              | 25-300                                    | 3-12                             |
| Cluster core  | 0.01   | < 1                                   | 10-30                                  | 10 <sup>4</sup>                | 3000                 | 1?   | 8     | < 80                               | > 8                              | 500-1500                                  | 1-3                              |
| Cluster relic   | 10 <sup>-4</sup>                             | < 1                                   | 1-5                                    | 10 <sup>6</sup> <sup>d</sup>   | 1000                 | 1?   | 9     | < 80 <sup>d</sup>                  | > 8                              | 3-15                                      | 15-33                            |
| IGM filament  | 5 10 <sup>-6</sup>                           | < 0.1                                 | < 0.3                                  | 5 10 <sup>6</sup> <sup>d</sup> | 5 10 <sup>5</sup>    | 1?   | 10    | < 2 <sup>d</sup>                   | > 50 <sup>e</sup>                | < 2                                       | > 40 <sup>e</sup>                |
| <b>Faraday-rotating, non-emitting media ("Faraday screens")</b> |  |                                       |  |                                |                      |      |       |                                    |                                  |   |                                  |
| Local Milky Way (high latitude)                                 | 0.03   | 2                                     | 3                                      | 200                            | 50                   | 0.5  | 11    | 10                                 | 24                               | 10  | 18                               |
| Local Milky Way (low latitude)                                  | 0.05   | 2                                     | 5                                      | 3000                           | 50                   | 0.5  | 11    | 80                                 | 8                                | 80  | 6                                |
| IGM around radio lobes  | 0.001  | < 1                                   | 1-5                                    | 10 <sup>5</sup>                | 5-20 10 <sup>3</sup> | 1?   | 12,13 | < 80                               | > 8                              | 20-200                                    | 4-13                             |

<sup>a</sup> Predicted; consistent with observations where available

<sup>b</sup> Optimum wavelength in case of differential Faraday rotation

<sup>c</sup> Optimum wavelength in case of internal Faraday dispersion

<sup>d</sup> Projection dependent

<sup>e</sup> Limited by the polarized emission of the Galactic foreground

**References:** 1: Fletcher et al. (2004), 2: Beck (2007), 3: Fletcher et al. (2011), 4: Hummel et al. (1991), 5: Heesen et al. (2009), 6: Kim et al. (1990), 7: Murgia et al. (2004), 8: Vogt & Enßlin (2005), 9: van Weeren et al. (2010), 10: Xu et al. (2006), 11: Sun & Reich (2009), 12: Laing et al. (2008), 13: Feain et al. (2009)